A Method for Modeling and Testing Modular Multilevel Converters and Their Controls in Large Power System Simulation Studies

J. Rupasinghe, S. Filizadeh
University of Manitoba
Canada

D. Muthumuni
Manitoba Hydro International
Canada

SUMMARY

In this paper, an average-value MMC model is developed using the concept of dynamic phasors. This model is capable of retaining the low-frequency dynamics of the converter, key harmonic components of the arm currents, and average submodule voltages. The developed model is particularly suited when an MMC is to be modeled in the context of a large power system in a co-simulation environment. The paper also develops a novel method for modeling and testing nonlinear converter control blocks that are prohibitively difficult to implement in an average-value model due to the ignored details of harmonic behaviour of internal waveforms. A specific contribution of the paper is the demonstration that important time-domain instantaneous measurements, for example, phase measurements from the PLL, can be combined with dynamic phasor techniques to obtain accurate dynamic and control results. The developed interface facilitates connecting not only complicated control blocks but also those that are black-boxed by the converter manufacturer.

The proposed modeling and co-simulation approach enables (i) creation of models of large power systems with multiple converter model types, (ii) direct testing of custom, proprietary, and complicated converter control systems, and (iii) use of multiple simulation time-steps (small time-steps for the EMT models and large time-steps for the average-value ones). The control scheme and the electrical network are implemented in the PSCAD/EMTDC simulator while the MMC is modelled in an external dynamic phasor solver. The MMC model's response to time-domain control system and the overall simulation accuracy are tested. The results demonstrate the effectiveness of the method in retaining key transient details and testing performances of control schemes using multi-rate co-simulation.

KEYWORDS

Co-simulation, Dynamic Phasor, Electromagnetic Transient (EMT) Simulation, Modular Multilevel Converter (MMC).

I. INTRODUCTION

Dynamic studies of modular multilevel converter (MMC) based networks are normally carried out using simulations based on detailed switching-type models that are commonly available in industrial-grade electromagnetic transient (EMT) simulation programs. These models are computationally demanding, and therefore massively time-consuming, as a large number of switching events need to be handled numerically. With the proliferation of renewable resources and formation of dc grids, such converter-intensive systems are on the rise; therefore, specialized simulation methods are necessary.

Detailed equivalent models [1] available in many EMT simulators offer marked reduction in computations, but do not greatly facilitate the simulation of large power systems wherein a large number of MMCs exist. Average-value converter models [2]–[7] that require much less computations are capable of representing low-frequency transient details with an adequate level of accuracy. However, majority of these models do not consider the behaviour of the submodules (SMs) of the MMC; hence, internal dynamic performances cannot be investigated. This shortcoming hinders the use of such models in testing controller schemes such as circulating current suppression control (CCSC) [8]; therefore, they are mostly used only in system-level dynamic studies.

Another way to achieve simulation efficiency is to use co-simulation [9], [10]. In this approach parts of the network in which details need to be retained are represented using EMT models, and the rest of the network is modeled using less detailed models, often in a distinct external solver. This permits to use efficient numerical techniques, multiple simulation time-steps, and parallel processing to speed up the simulation. However, these models require implementation of specialized control mechanisms that control the system-level and internal dynamics of the MMC, which are immensely difficult in co-simulation settings.

In this paper, an MMC average-value model with the ability to study internal waveforms is developed using dynamic phasor (DP) principles. The benefits of the modeling technique and the solution procedure are enhanced by developing the model outside the EMT solver such that the model can be solved with an adequately larger time-step than the rest of the electrical network. Then the model is further extended by introducing novel means to control the internal and system-level dynamics using control schemes implemented inside the EMT solver.

II. MATHEMATICAL MODEL OF AN MMC

An MMC is a multi-cell converter topology, which is built by stacking a large number of identical SMs in each arm [11]. An arm acts as a variable voltage source, which allows to synthesize an approximately sinusoidal waveform at its AC output by regulating the number of inserted SMs in the conduction path of the arm. Figure 1 illustrates a three-phase representation of a common half-bridge MMC configuration and the structure of a SM. A SM capacitor may be inserted in the arm or bypassed to construct the arm voltage level by switching its IGBTs.

Consider a general phase of MMC in Figure 1, which consists of N SMs per arm. Expressions that describe the upper (u) and lower (l) capacitor voltages and arm currents of an arbitrary phase $j = a$, b, c are as follows.

$$\frac{d}{dt}V_{SM,j}^{u} = \frac{\lambda_{j}^{u}}{C_{SM}N}i_{j}^{u} \tag{1}$$

$$\frac{d}{dt}V_{SM,j}^{l} = \frac{\lambda_{j}^{l}}{C_{SM}N}i_{j}^{l} \tag{2}$$

$$\frac{d}{dt}i_{j}^{u} = \frac{V_{dc}}{2L} - \frac{1}{L}\lambda_{j}^{u}V_{SM,j}^{u} - \frac{R}{L}i_{j}^{u} - \frac{1}{L}v_{j} \tag{3}$$

$$\frac{d}{dt}i_{j}^{l} = \frac{V_{dc}}{2L} - \frac{1}{L}\lambda_{j}^{l}V_{SM,j}^{l} - \frac{R}{L}i_{j}^{l} - \frac{1}{L}v_{j} \tag{4}$$

where $V_{SM,j}^{u,l}$, $i_{j}^{u,l}$, V_{dc}, v_{j}, and $\lambda_{j}^{u,l}$ are average SM voltage, arm current, dc bus voltage, ac phase voltage, and capacitor switching function, respectively. The capacitor switching function, which is a function of modulation index (m), power angle (δ), and the phase angle (θ) of the point of common coupling, characterises the number of inserted SMs in the arm during each switching state. It is derived assuming
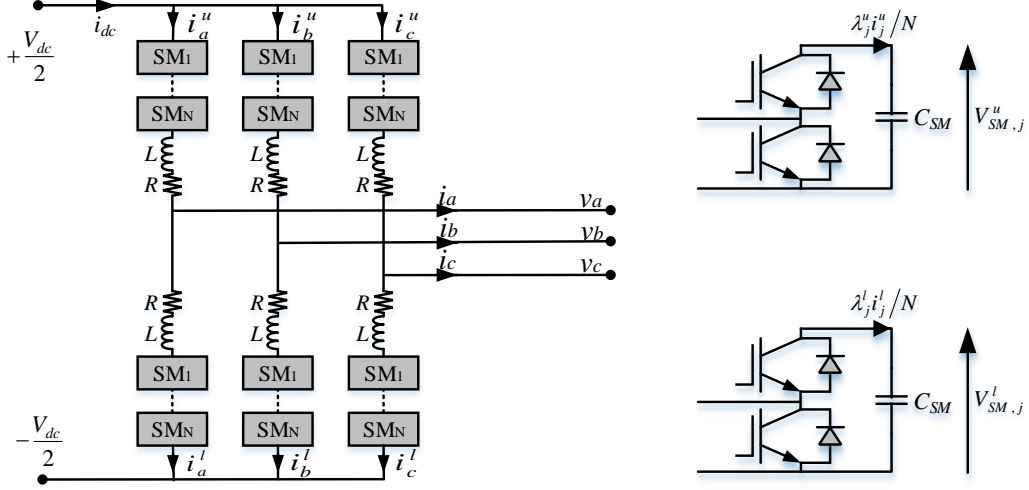
Figure 1. MMC and SM configuration

that all SM capacitor voltages are balanced and equal to their nominal voltage and that the output of the MMC is perfectly sinusoidal at fundamental frequency.

$$\lambda_j^u = \frac{N}{2}(1 - m.\sin(\theta + \delta)) \tag{5}$$

$$\lambda_j^l = \frac{N}{2}(1 - m.\sin(\theta + \delta)) \tag{6}$$

For the convenient of identifying odd and even harmonics of variables distinctly, (1)-(6) are rewritten in terms of new variables defined by taking the summation (s) and the difference (d) of the upper and lower arm variables as below.

$$\frac{d}{dt}V_{SM,j}^s = \frac{1}{2NC_{SM}}\left(\lambda_j^s i_j^s + \lambda_j^d i_j^d\right) \tag{7}$$

$$\frac{d}{dt}V_{SM,j}^d = \frac{1}{2NC_{SM}}\left(\lambda_j^s i_j^d + \lambda_j^d i_j^s\right) \tag{8}$$

$$\frac{d}{dt}i_j^s = \frac{-1}{L}\left(\frac{1}{2}\lambda_j^s V_{SM,j}^s + \frac{1}{2}\lambda_j^d V_{SM,j}^d + Ri_j^s - V_{dc}\right) \tag{9}$$

$$\frac{d}{dt}i_j^d = \frac{-1}{L}\left(\frac{1}{2}\lambda_j^s V_{SM,j}^d + \frac{1}{2}\lambda_j^d V_{SM,j}^s + Ri_j^d - v_j\right) \tag{10}$$

$$\lambda_j^s = N \tag{11}$$

$$\lambda_j^u = -mN\sin(\theta + \delta) \tag{12}$$

It is important to note that all sum variables comprise of dc and even harmonics, and the difference variables encompass odd harmonics. The difference of the arm currents is equal to the MMC's output AC current, i_j.

III. DYNAMIC PHASOR MODELING OF MMC FOR DP-EMT CO-SIMULATIONS

A. Dynamic Phasor Basics

DPs are essentially the time-varying Fourier coefficients of a time-domain signal, which can be extracted using samples of the signal within a fixed window, which slides over time [12]. The nature of DP modeling allows to use larger time-steps for simulations compared to the time-domain EMT solutions as they yield a time-invariant model in steady state, thus relaxing the computational burden of the solution. Consider a time-domain signal $x(t)$ over the time interval ($t-T,t$], where T is the period of the signal and ω_0 is the fundamental angular frequency. The Fourier series of the signal is written as

$$x(t - T + s) = \sum_{h=-\infty}^{\infty} \langle x \rangle_h (t) e^{jh\frac{2\pi}{T}(t-T+s)} \tag{13}$$

where,

$$\langle x \rangle_h (t) = \frac{1}{T} \int_0^T x(t - T + s) e^{-jh\frac{2\pi}{T}(t-T+s)} ds \tag{14}$$

is the hth order DP of $x(t)$. It can be observed from (13) that DP provides the selectivity to include or exclude harmonics from the signal based on the desired level of accuracy. Some useful properties of DPs that prove useful in modelling applications are given below.

$$\frac{d}{dt} \langle x \rangle_h (t) = \left\langle \frac{d}{dt} x \right\rangle_h (t) - jh\frac{2\pi}{T} \langle x \rangle_h (t) \tag{15}$$

$$\langle x.y \rangle_h (t) = \sum_{i=-\infty}^{\infty} \langle x \rangle_{h-i} \langle y \rangle_i \tag{16}$$

B. Dynamic Phasor Modeling of MMC

The DP-MMC model for h^{th} order harmonic can be derived by applying DP properties to (7)-(12).

$$\frac{d}{dt} \left\langle V_{SM,j}^s \right\rangle_h = \frac{1}{2NC_{SM}} \left(\sum_{i=-\infty}^{\infty} \left\langle \lambda_j^s \right\rangle_{h-i} \left\langle i_j^s \right\rangle_i + \sum_{i=-\infty}^{\infty} \left\langle \lambda_j^d \right\rangle_{h-i} \left\langle i_j^d \right\rangle_i \right) - jh\omega_0 \left\langle V_{SM,j}^s \right\rangle_h \tag{17}$$

$$\frac{d}{dt} \left\langle V_{SM,j}^d \right\rangle_h = \frac{1}{2NC_{SM}} \left(\sum_{i=-\infty}^{\infty} \left\langle \lambda_j^s \right\rangle_{h-i} \left\langle i_j^d \right\rangle_i + \sum_{i=-\infty}^{\infty} \left\langle \lambda_j^d \right\rangle_{h-i} \left\langle i_j^s \right\rangle_i \right) - jh\omega_0 \left\langle V_{SM,j}^d \right\rangle_h \tag{18}$$

$$\frac{d}{dt} \left\langle i_j^s \right\rangle_h = \frac{-1}{2L} \left(\sum_{i=-\infty}^{\infty} \left\langle \lambda_j^s \right\rangle_{h-i} \left\langle V_{SM,j}^s \right\rangle_i + \sum_{i=-\infty}^{\infty} \left\langle \lambda_j^d \right\rangle_{h-i} \left\langle V_{SM,j}^d \right\rangle_i \right) - \left(\frac{R}{L} + jh\omega_0 \right) \left\langle i_j^s \right\rangle_h - \frac{1}{L} \left\langle V_{dc} \right\rangle_h \tag{19}$$

$$\left\langle v_j \right\rangle_h = \frac{-1}{4} \left(\sum_{i=-\infty}^{\infty} \left\langle \lambda_j^s \right\rangle_{h-i} \left\langle V_{SM,j}^d \right\rangle_i + \sum_{i=-\infty}^{\infty} \left\langle \lambda_j^d \right\rangle_{h-i} \left\langle V_{SM,j}^s \right\rangle_i \right) - \left(\frac{R + jh\omega_0}{2} \right) \left\langle i_j^d \right\rangle_h - \frac{L}{2} \frac{d}{dt} \left\langle i_j^d \right\rangle_h \tag{20}$$

$$\left\langle \lambda_j^s \right\rangle_h = \begin{cases} N & \text{if } h = 0 \\ 0 & \text{otherwise} \end{cases} \tag{21}$$

$$\left\langle \lambda_j^d \right\rangle_h = \begin{cases} j\frac{mN}{2} e^{j\delta} & \text{if } h = 1 \\ 0 & \text{otherwise} \end{cases} \tag{22}$$

Equations (17)-(19) must be solved using a numerical integration technique to find the SM voltages and arm current considering only the important harmonics of each variable. For example, dc and the second order terms are computed for sum variables while the first order component is computed for difference variables. Then the output voltage of the MMC is computed by solving (20). For that, DPs of the output current must be extracted. This can be readily done employing (14). Once the ac side and internal dynamics are calculated, the dc output is obtained as

$$\left\langle i_{dc} \right\rangle_0 = \sum_{j=a,b,c} \left\langle i_j^s \right\rangle_0 / 2 \tag{23}$$

This model provides a means to control the system-level behaviour of the MMC by controlling the modulation index, m, and the power angle, δ. However, the model does not provide the required degree of freedom to control internal dynamics such as circulating currents. This can be remedied by making changes to the capacitor switching function.

C. MMC Control

The control scheme of an MMC can be mainly categorized into primary control, secondary control, and balancing control [8], [11]. The primary controller includes control of system-level parameters such as real power and reactive power (or bus voltage). This can be readily done by controlling the modulation index and the power angle of the MMC. The secondary control system may include schemes such as circulating current suppression control (CCSC), capacitor ripple control, and MMC energy control. The balancing algorithm ensures that SM voltages are kept around the nominal value. However, balancing

control is not considered in this paper as the DP-MMC model is based on the assumption that all the SM voltages are balanced. A modulation technique such as nearest level control (NLC) [13] is included at the end of the control system to determine the number of SMs to be inserted to the arm in each switching state. The MMC output is synchronize with the ac network by adding a phase locked loop (PLL), which measures the phase angle at the point of common coupling of the MMC.

D. Improving the Model to Test Time-Domain Control Systems

The switching function given in (5) and (6) are built upon two main assumptions, namely (i) the output of the converter has a single frequency, i.e., no harmonics exist in the output, and (ii) no secondary control system is implemented to control the MMC. However, this is not the case in virtually all real world applications; thus, a sophisticated method is required to rectify this problem.

Consider an MMC control system, which includes both the primary and the secondary controllers. The overall control signal produced by the controller for the upper and lower arms may be given as,

$$S_j^u = 1 - v_{ref,j} + u_{z,j} \tag{24}$$

$$S_j^l = 1 + v_{ref,j} + u_{z,j} \tag{25}$$

where $v_{ref,j}$ is the output signal produced by the primary controller in per unit and $u_{z,j}$ is the control signal generated by the secondary controller in per unit. Note that if the output of the MMC is expected to be perfectly sinusoidal at the fundamental frequency, the $v_{ref,j}$ term can be replaced with $m.\sin(\theta+\delta)$. The number of SMs to be inserted in the arm at a given instance - in other words the switching function - can be derived by multiplying the control signal by the base voltage, $V_{dc}/2$, and then dividing it by nominal SM voltage:

$$\lambda_j^u = \frac{N}{2} S_j^u = \frac{N}{2} \left(1 - v_{ref,j} + u_{z,j}\right) \tag{26}$$

$$\lambda_j^l = \frac{N}{2} S_j^l = \frac{N}{2} \left(1 + v_{ref,j} + u_{z,j}\right) \tag{27}$$

The DPs of the switching function can be given after taking the summation and the difference of upper and lower arm switching functions as below.

$$\left\langle \lambda_j^s \right\rangle_h = \frac{N}{2} \left\langle S_j^s \right\rangle_h = \begin{cases} N + \left\langle u_{z,j} \right\rangle_0 & \text{if } h = 0 \\ \left\langle u_{z,j} \right\rangle_h & \text{otherwise} \end{cases} \tag{28}$$

$$\left\langle \lambda_j^d \right\rangle_h = \frac{N}{2} \left\langle S_j^d \right\rangle_h = -N \left\langle v_{ref,j} \right\rangle_h \tag{29}$$

The primary control signal, $v_{ref,j}$, is generally made up of odd harmonics. If the MMC has a large number of voltage levels, it is sufficiently accurate to only compute the fundamental DP component of $\left\langle \lambda_j^d \right\rangle_h$ as the output is expected to be nearly sinusoidal. Secondary controllers such as CCSC produce second-order harmonics of $u_{z,j}$. Therefore, computing the dc term ($h = 0$) and the second-order term ($h = 2$) of $\left\langle \lambda_j^s \right\rangle_h$ is sufficient. It is important to note that in this derivation the switching function for the DP-MMC model is extracted using the time-domain control signals. Therefore, this provides a means to test a given control system using the DP-MMC model without further modification to the MMC or the control system. In a situation where the control signal passes through a modulator such as NLC, the overall control signal may contain more harmonics; therefore, more harmonics of the switching function need to be considered for satisfactory accuracy.

E. Model Interface to an EMT Solver

Modeling with DP relocates the frequency spectrum of a signal from its fundamental operating frequency to around zero. This reduces the computational effort needed for simulating DP quantities by allowing appropriately large time-steps for the model solution. In order to take advantage of this feature,
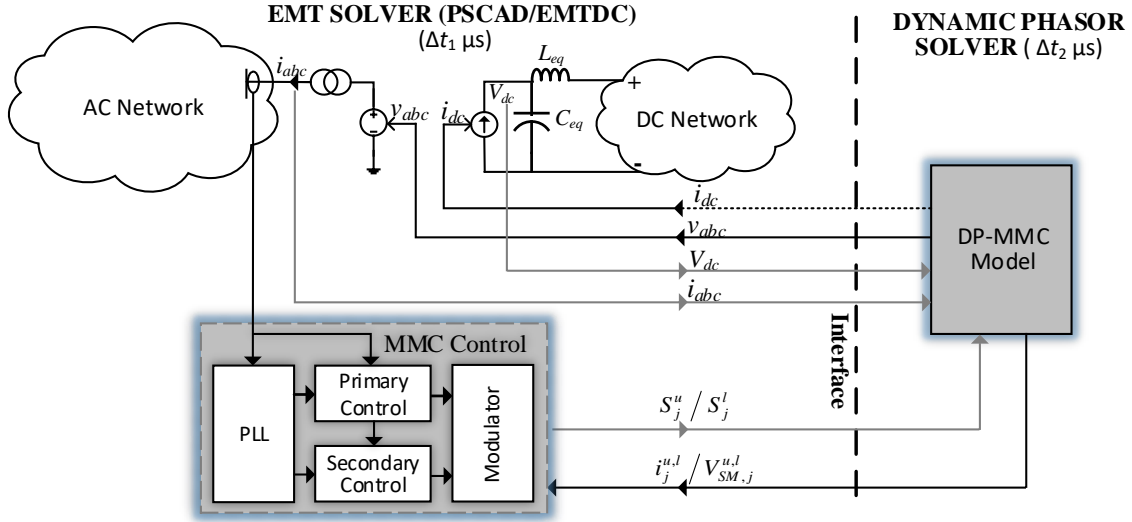
Figure 2: MMC model interface to the EMT solver

the MMC model is implemented in a distinct DP solver in such a way that it can be solved with a larger time-step than the rest of the electrical network and the MMC control system, which are built in the context of an EMT solver. This is illustrated in Figure 2.

As shown in the Figure 2, the MMC model is interfaced to the ac and dc electrical networks via a controlled three-phase voltage source and a controlled current source, respectively. The values of these sources are updated in each time-step by communicating the values computed by the MMC model in the DP solver after converting them to time-domain. Control signals that are generated by the control system based on the feedback from the network and the MMC model, line currents, and the dc voltage are communicated back to the DP solver for use in the next time-step solution. In addition to the controlled current source, the dc side is accompanied by a shunt capacitor ($C_{eq} = 6C_{SM} / N$) and a series inductance ($L_{eq} = 2L/3$) to mimic the effect of energy stored in SM capacitors and the effect of arm inductance on dc current path, respectively [6].

IV. MODEL VALIDATION

An MMC connected ac system, which is shown in Figure 3(a), is co-simulated using the proposed DP-MMC model and PSCAD/EMTDC to validate the accuracy. PSCAD/EMTDC [14] is a well-established
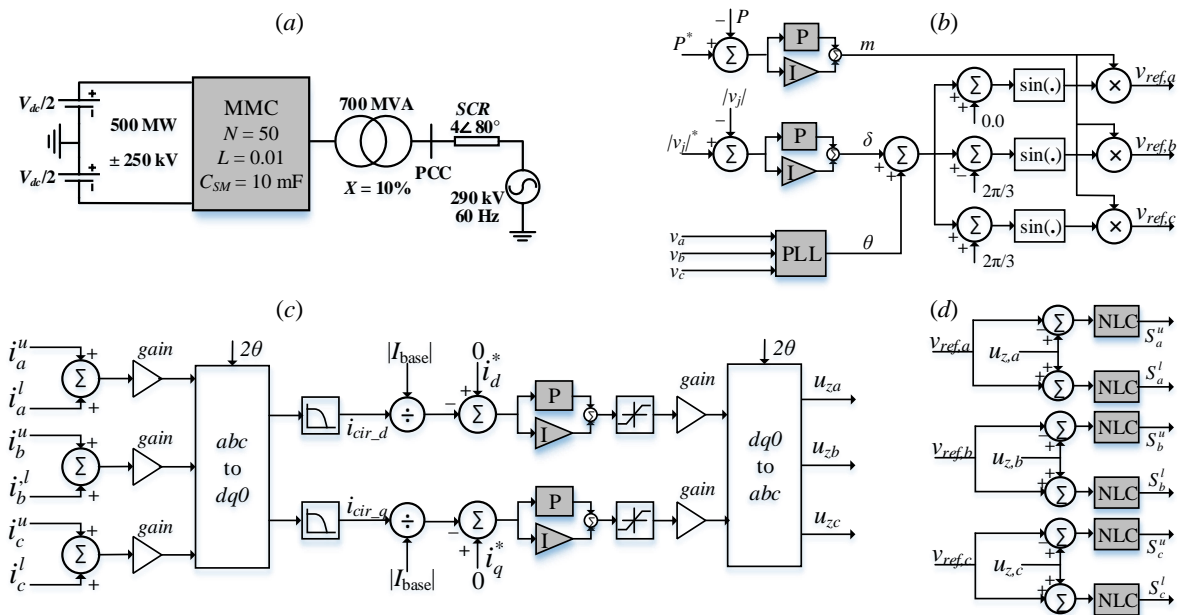

Figure 3: MMC test system and the controllers; (a) MMC connected ac system, (b) primary controller,

5

industrial grade EMT-type simulator used in power system transient studies, which consists of a library of electrical and control components. A primary control system (see Figure 3(b)) to regulate the MMC's output power and ac voltage magnitude, and a secondary control scheme (see Figure 3(c)) to suppress circulating currents of the arms are added. The electrical network, except the MMC model, and the control system are implemented in PSCAD/EMTDC using standard inbuilt library components. The DP-MMC is developed in an external application using C++. The dc ($h = 0$) component, fundamental component ($h = 1$), and the second order component ($h = 2$) of the switching function are considered for the control of MMC. The communication between PSCAD/EMTDC and the DP solver is established via an inbuilt co-simulation module of PSCAD/EMTDC. Solution time-steps of 200 µs and 50 µs are used for DP solver and PSCAD/EMTDC, respectively.

A. System Controller Response (without CCSC)

The MMC models' response to a step change in power reference form 500 MW to 350 MW at $t = 5.0$ s is shown in Figure 4. For the purpose of validating the accuracy of the DP-MMC model, results are compared by modeling and simulating the entire system in PSCAD/EMTDC using a detailed equivalent MMC model [1]. It can be seen that the system dynamics and MMC internal dynamics closely match those of the PSCAD/EMTDC waveforms. There are slight mismatches in internal waveforms due to the consideration of small amount of harmonics. Accuracy of those waveforms can be improved by including more harmonics in the DP solution but with an increased amount of computations.

B. CCSC Controller Response

The effectiveness of the proposed strategy to include secondary control systems in a DP-MMC model is well illustrated in Figure 5. The simulation is initiated without the CCSC and then it is enabled at $t = 5.0$. Figure 5 shows a significant reduction of arm's second-order circulating current. As a result, a marked improvement is visible in the arm current waveform. This can be further validated by analysing the harmonic spectrum of the arm current as given in Figure 6. It shows a clear cut down of the magnitude of the second-order current component after enabling CCSC while the magnitudes of other harmonic components stay almost the same.
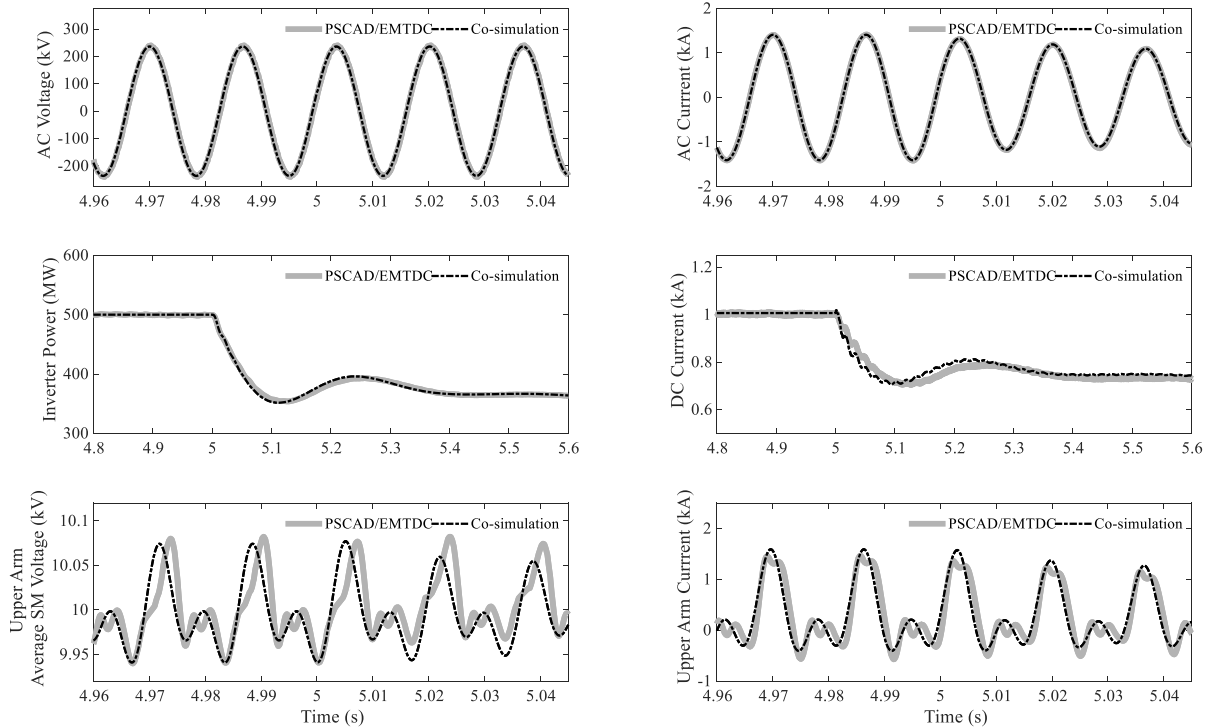

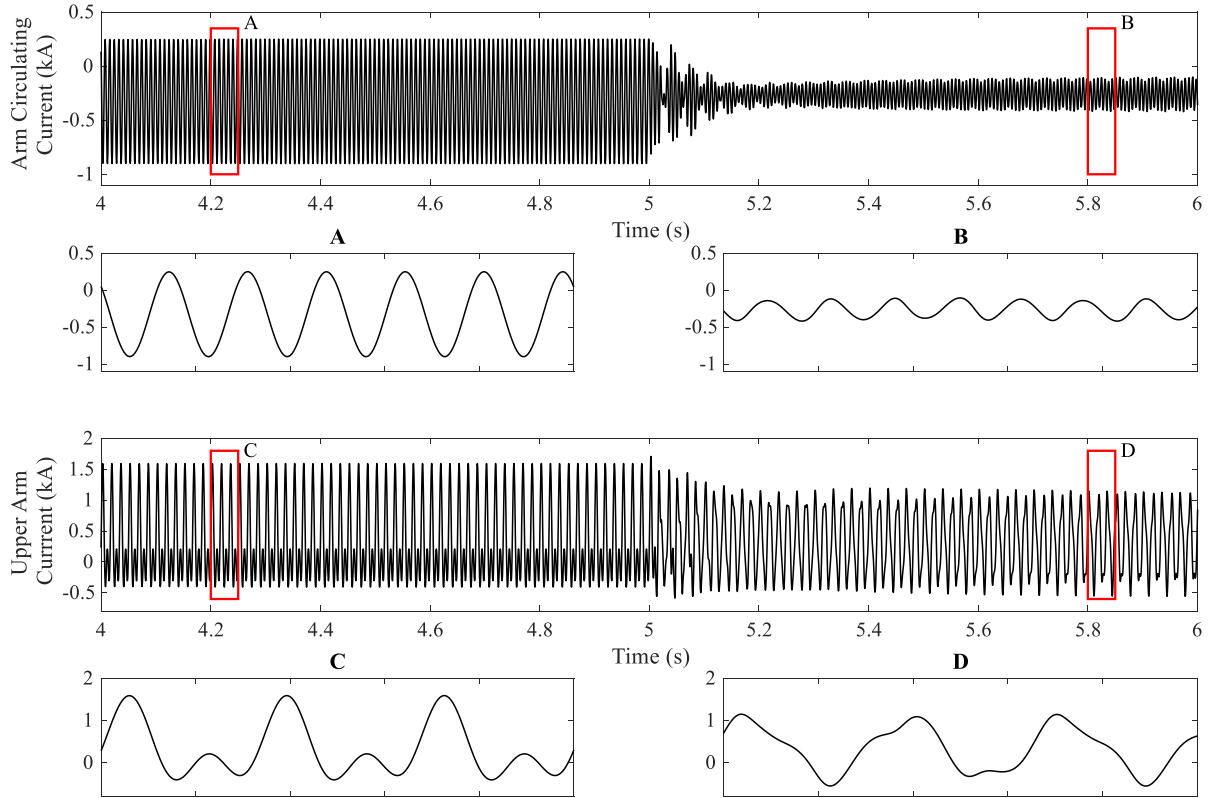Figure 4: MMC response to a power order change from 500 MW to 350 MW

6

Figure 5: CCSC response of DP-MMC model; CCSC is enabled at $t = 5.0$.
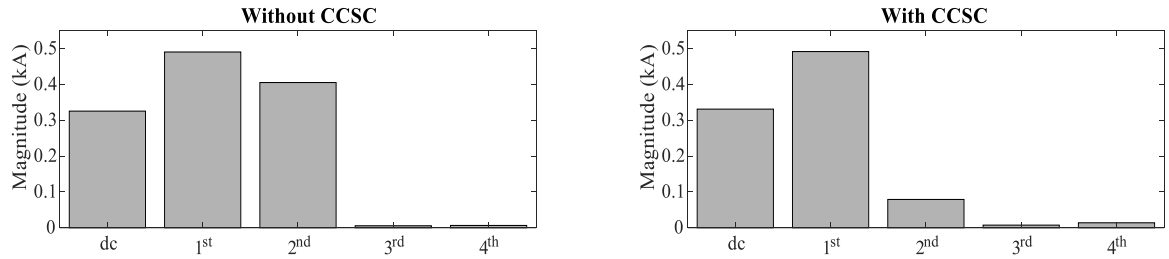

Figure 6: Harmonic spectrum of arm current with and without CCSC.

V. CONCLUSION

An MMC model was developed in this paper using DP principles for EMT-DP co-simulation of large power systems. The model was implemented in an external DP solver; a novel method to interface it to an EMT solver was introduced. This paper also devised a state-of-the-art technique to test primary and secondary MMC control schemes, which are extremely difficult to implement in a DP environment, employing control blocks available in EMT simulators. This approach brings benefits in studying complicated or black-boxed control strategies, for example, proprietary control schemes from vendors, as the DP-MMC model can be readily simulated just by replacing the control system with any given configuration. Simulation results obtained by developing a co-simulation platform using DP-MMC model and PSCAD/EMTDC verified the accuracy and effectiveness of the overall scheme.

BIBLIOGRAPHY

[1] U. N. Gnanarathna, A. M. Gole, and R. P. Jayasinghe, "Efficient Modeling of Modular Multilevel HVDC Converters (MMC) on Electromagnetic Transient Simulation Programs," *IEEE Trans. Power Deliv.*, vol. 26, no. 1, pp. 316–324, Jan. 2011.

[2] H. Saad *et al.*, "Modular Multilevel Converter Models for Electromagnetic Transients," *IEEE Trans. Power Deliv.*, vol. 29, no. 3, pp. 1481–1489, Jun. 2014.

[3] J. Peralta, H. Saad, S. Dennetiere, J. Mahseredjian, and S. Nguefeu, "Detailed and Averaged Models for a 401-Level MMC–HVDC System," *IEEE Trans. Power Deliv.*, vol. 27, no. 3, pp. 1501–1508, Jul. 2012.

[4] H. Saad *et al.*, "Dynamic Averaged and Simplified Models for MMC-Based HVDC Transmission Systems," *IEEE Trans. Power Deliv.*, vol. 28, no. 3, pp. 1723–1730, Jul. 2013.

[5] J. Xu, C. Zhao, W. Liu, and C. Guo, "Accelerated Model of Modular Multilevel Converters in PSCAD/EMTDC," *IEEE Trans. Power Deliv.*, vol. 28, no. 1, pp. 129–136, Jan. 2013.

[6] J. Rupasinghe, S. Filizadeh, and L. Wang, "A Dynamic Phasor Model of an MMC With Extended Frequency Range for EMT Simulations," *IEEE J. Emerg. Sel. Top. Power Electron.*, vol. 7, no. 1, pp. 30–40, Mar. 2019.

[7] J. Xu, A. M. Gole, and C. Zhao, "The Use of Averaged-Value Model of Modular Multilevel Converter in DC Grid," *IEEE Trans. Power Deliv.*, vol. 30, no. 2, pp. 519–528, Apr. 2015.

[8] Q. Tu, Z. Xu, and L. Xu, "Reduced Switching-Frequency Modulation and Circulating Current Suppression for Modular Multilevel Converters," *IEEE Trans. Power Deliv.*, vol. 26, no. 3, pp. 2009–2017, Jul. 2011.

[9] D. Shu, X. Xie, Q. Jiang, G. Guo, and K. Wang, "A Multirate EMT Co-Simulation of Large AC and MMC-Based MTDC Systems," *IEEE Trans. Power Syst.*, vol. 33, no. 2, pp. 1252–1263, Mar. 2018.

[10] X. Meng and L. Wang, "Interfacing an EMT-type modular multilevel converter HVDC model in transient stability simulation," *Transm. Distrib. IET Gener.*, vol. 11, no. 12, pp. 3002–3008, 2017.

[11] M. A. Perez, S. Bernet, J. Rodriguez, S. Kouro, and R. Lizana, "Circuit Topologies, Modeling, Control Schemes, and Applications of Modular Multilevel Converters," *IEEE Trans. Power Electron.*, vol. 30, no. 1, pp. 4–17, Jan. 2015.

[12] S. R. Sanders, J. M. Noworolski, X. Z. Liu, and G. C. Verghese, "Generalized averaging method for power conversion circuits," *IEEE Trans. Power Electron.*, vol. 6, no. 2, pp. 251–259, Apr. 1991.

[13] P. M. Meshram and V. B. Borghate, "A Simplified Nearest Level Control (NLC) Voltage Balancing Method for Modular Multilevel Converter (MMC)," *IEEE Trans. Power Electron.*, vol. 30, no. 1, pp. 450–462, Jan. 2015.

[14] "Overview | PSCAD." https://www.pscad.com/software/pscad/overview (accessed May 28, 2020).